MAGMATIC EPISODES IN THE HOLY CROSS MOUNTAINS, POLAND – A NEW CONTRIBUTION FROM MULTI-AGE ZIRCON POPULATIONS

EPIZODY MAGMOWE W GÓRACH ŚWIĘTOKRZYSKICH – NOWE DANE O POPULACJACH CYRKONU RÓŻNEGO WIEKU

Ewa Krzemińska[1], Leszek Krzemiński[1]

Abstract. This contribution reports on new U-Pb zircon age data from magmatic rocks from the Holy Cross Mountains (HCM) of Poland. The analyzed samples were taken from lamprophyre and diabase veins of Podkranów and Janowice-2 as well as from tuff horizon of Kielce Beds (Ludlow). Internal morphologies have been investigated by SEM-BSE and cathodoluminescence images and they have been used as a guide for the selection of genetically various type of grains, *e.g.* potential auto-, ante- and xenocrysts, that were analyzed by ion microprobe. The U-Pb age of the magmatic events at 414.2 ±6.6 Ma (Kielce tuff), 322 ±12 Ma (Podkranów, lamprophyre), and 300±10 Ma (Janowice-2, diabase) confirmed the time frame of known magmatic activity reported within the HCM, as determined by ^{40}Ar/^{39}Ar geochronology in previous studies. The zircon investigation revealed also multiple populations with record of an earlier pulse of magma system (antecrysts), as well as abundant xenocrysts.

Key words: U-Pb geochronology, zircon, antecrysts, xenocrysts, diabase, lamprophyre, tuff, Łysogóry Region, Kielce Region.

Abstrakt. W artykule przedstawiono nowe oznaczenia wieku U-Pb cyrkonu w skałach magmowych z obszaru Gór Świętokrzyskich (HCM). Próbki pobrano z żył lamprofiru i diabazu z Podkranowa i Janowic-2 oraz z poziomu tufu w warstwach kieleckich (ludlow). Morfologię i wewnętrzne cechy budowy ziaren zbadano za pomocą obrazów SEM-BSE i katodoluminescencji SEM, stosując je jako przewodnik do selekcji genetycznie różnych typów ziaren, potencjalnych auto-, ante- i ksenokryształów, które były analizowane na mikrosondzie jonowej. Wiek U-Pb epizodów magmowych, 414,2 ±6,6 Ma (Kielce, tuf), 322 ±12 Ma (Podkranów, lamprofir) i 300 ±10 Ma (Janowice-2, diabaz), potwierdza znane z wcześniejszych publikacji ramy czasowe aktywności magmowej na obszarze HCM oznaczone metodą ^{40}Ar/^{39}Ar. Badania wieku U-Pb cyrkonu ujawniły także szereg populacji z zapisem wcześniejszych impulsów magmowych (antekryształy) i licznych ksenokryształów.

Słowa kluczowe: geochronologia U-Pb, cyrkon, antekryształy, ksenokryształy, diabaz, lamprofir, tuf, region łysogórski, region kielecki.

INTRODUCTION

Within the Paleozoic sedimentary succession of the Holy Cross Mountains (HCM) in Poland, there are a several magmatic horizons (Fig. 1), represented by diabase and lamprophyre dykes or tuff layers (*e.g.*, Czarnocki, 1919; Ryka, 1957; Kardymowicz, 1967). They form important chronostratigraphic markers and they can be used for correlating sedimentary and volcanic deposits. The timing of a few of magmatic events has been already established using the

^{40}Ar/^{39}Ar thermochronology, interpreted as an emplacement age of each diabase dyke (Nawrocki *et al.*, 2007, 2013). Ar/Ar ages for such unmetamorphosed subvolcanic and volcanic systems are commonly accepted as a time of the emplacement event (Kelley, 2002).

U-Pb zircon geochronology, with closure temperatures above critical felsic magmatic crystallization temperatures at *c.* 800°C is more robust technique, also frequently employed to obtain an age of these specific magmatic rocks. The zircon data from such rocks, however, do not always demonstrate

---

[1] Polish Geological Institute – National Research Institute, 4 Rakowiecka Street, 00-975 Warsaw, Poland; e-mail: ewa.krzeminska@pgi.gov.pl, leszek.krzeminski@pgi.gov.pl.
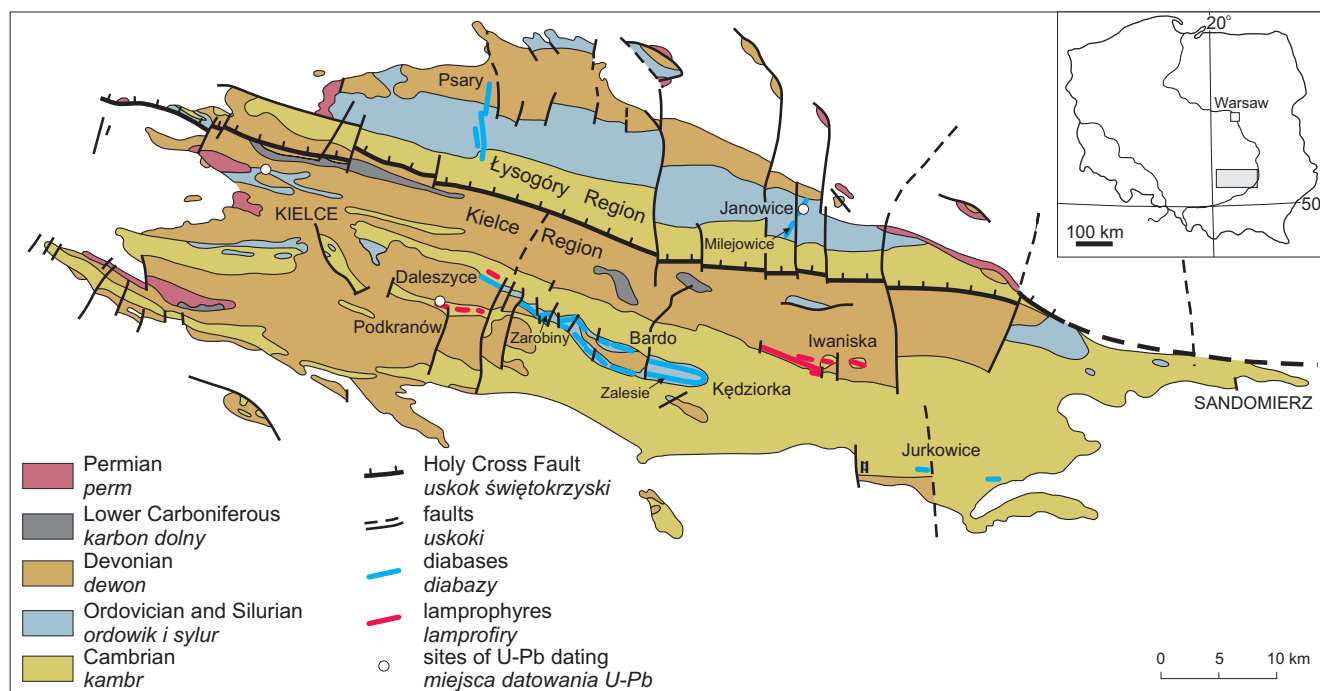
Fig. 1. Simplified geological map of Paleozoic rocks in the Holy Cross Mountains (after Kowalczewski, 2004), with the localities of sampled tuff, diabase, and lamprophyre

Uproszczona mapa geologiczna utworów paleozoicznych w Górach Świętokrzyskich (wg Kowalczewskiego, 2004) z lokalizacją próbek tufu, diabazu i lamprofiru

a well-defined, single data population, containing many zircon groups, which require a careful interpretation of the age data, but if exist they provide much more information than emplacement or/and eruption age. The samples from volcanic or subvolcanic rocks usually include antecrysts, defined as zircon grains that crystallized from an earlier pulse of magma, and which were incorporated in later pulses (Miller *et al.*, 2007 and references therein), and inherited components *e.g.* xenocrysts, which can complicate interpretation of the U-Pb isotopic data. The antecrysts and xenocrysts may provide however a useful information on different magmatic events, or host rocks provenance. This paper reports the first use of the U-Pb sensitive ion microprobe SHRIMP II technique on zircons from magmatic rocks of the HCM area.

The area of HCM is tectonically complex, divided by Holy Cross Fault (Fig. 1) into the two regions Łysogóry in the north and the Kielce in the south, belonging to Małopolska Block. They display several stratigraphic and tectonic differences, that have generated a long-lasting debate as to whether the Łysogóry and Małopolska blocks shared a common pre-Devonian tectonic evolution or evolved independently (*e.g.*, Belka *et al.*, 2002; Nawrocki *et al.*, 2007; Kozłowski *et al.*, 2014; Walczak, Belka, 2017). Assuming the juxtaposition of Małopolska against Łysogóry in the Silurian, it should result in the amalgamation and synchronicity of magmatic events or/and identity of the detritus between the domains. Thus the zircon age study including exploration of pre-eruptive or pre-emplacement history of grains and examination of synchronicity of magmatic acti-

vity seems to be further contribution to this discussion. The zircon grains for U-Pb geochronology were selected from rocks derived from both of regions. They represent Łysogóry Region, with sample taken from Janowice diabase (~50°50′55″N, 21°14′52″E) as well as from Kielce Region from Podkranów lamprophyre (50°50′55″N, 21°14′52″E) and from tuff (a thin volcanic ash layer) from Kielce (50°89′79″N, 20°61′38″E).

OVERVIEW OF PREVIOUS AGE DETERMINATIONS

Radiometric age results for igneous rocks in HCM area do not form a large collection, owing to limited suitable samples, that allowed to K-Ar and ^{40}Ar/^{39}Ar geochronology studies. An overview is presented in Table 1. It contains a record of episodes documented mostly in Kielce Region, and just a few from Łysogóry Region, highlighting the fact the HCM area is situated in two distinct crustal blocks: northern – Łysogóry and southern – Małopolska (where Kielce Region is included), that differ in age of Paleozoic magmatic activity as well as the contrasting lithofacies, stratigraphy and tectonic development during early Paleozoic times (*e.g.*, Dadlez, 2001; Narkiewicz *et al.*, 2011; Walczak, Belka, 2017).

The most of age results (Table 1) with relatively more precise ^{40}Ar/^{39}Ar data have focused on potassium rich biotite and whole-rock option most appropriate for fine-grained diabase. The plagioclase has rarely been used as a chronometer,

<div align="right">**Table 1**</div>

The outline of published radiometric age data for magmatic rocks from the Łysogóry and Kielce Regions

Przegląd publikowanych danych dotyczących wieku radiometrycznego skał magmowych z regionów łysogórskiego i kieleckiego

Site	Lithology	Material	Łysogóry Region		Kielce Region		Geochronologic epoch[2]	Reference
			Method	Age (Ma)	Method	Age (Ma)		
Wzorki-1 (72.4 m)	diabase	whole rock	Ar/Ar plateau	242.7 ±1.6[1]			Middle Triassic	Nawrocki *et al.* (2013)
Wzorki-1 (72.4 m)	diabase	whole rock	Ar/Ar plateau	243.0 ±2[1]			Middle Triassic	Nawrocki *et al.* (2013)
Prągowiec	diabase	plagioclase			Ar/Ar plateau	254.5 ±12	Lopingian (P$_3$)	Migaszewski (2002)
Wszachów-4 (81.0 m)	lamprophyre	biotite			K-Ar	275.0 ±15	Cisuralian (P$_1$)	Migaszewski (2002)
Wszachów-4 (74.0 m)	lamprophyre	biotite			K-Ar	288.8 ±15	Cisuralian (P$_1$)	Migaszewski (2002)
Janowice-2 (61–69 m)	diabase	zircon	U-Pb	300.0 ±10			Late Pennsylvanian	this study
Kolonia-2 (122.0 m)	lamprophyre	biotite			K-Ar	311.5 ±15	Middle Pennsylvanian	Migaszewski (2002)
Podkranów	lamprophyre	zircon			U-Pb	322.0 ±12	Early Pennsylvanian	this study
Milejowice-1 (96.4 m)	diabase	whole rock	Ar/Ar plateau	322.5 ±1.1			Early Pennsylvanian	Nawrocki *et al.* (2013)
Milejowice-1 (96.4 m)	diabase	whole rock	Ar/Ar plateau	331.0 ±1.9			Middle Mississippian	Nawrocki *et al.* (2013)
Góra Salkowa	lamprophyre	biotite			K-Ar	347.8 ±15	Early Mississippian	Migaszewski (2002)
Kolonia-2 (140.1 m)	lamprophyre	biotite			K-Ar	351.2 ±15	Early Mississippian	Migaszewski (2002)
Wszachów-4 (81.0 m)	lamprophyre	biotite			K-Ar	374.4 ±15	Late Devonian	Migaszewski (2002)
Zalesie	diabase	plagioclase			K-Ar	391.7 ±19	Middle Devonian	Migaszewski (2002)
Zarobiny PIG 1 (84.8 m)	diabase	whole rock			Ar/Ar plateau	412.0 ±2	Early Devonian	Nawrocki *et al.* (2013)
Zarobiny PIG 1 (84.8 m)	diabase	whole rock			Ar/Ar plateau	415.0 ±2	Early Devonian	Nawrocki *et al.* (2013)
Kielce	tuff	zircon			U-Pb	414.5 ±6.6 / 425.7 ±6.6	Early Devonian Ludlow	this study
Zalesie	diabase	plagioclase			Ar/Ar plateau	424.0 ±6	Ludlow	Nawrocki *et al.* (2007)

[1] Most probably secondary age defining hydrothermal alteration (Nawrocki *et al.*, 2013) / najprawdopodobniej wtórny wiek datujący zmiany hydrotermalne (Nawrocki i in., 2013)

[2] Adapted from Cohen *et al.*, 2013 (updated) / na podstawie pracy Cohena i in., 2013 (zaktualizowane)

largely due to quantifying argon diffusion kinetics from a mineral with low-K concentration. These diffusion parameters correspond to closure temperatures of 225–300°C (Cassata *et al.*, 2009). In case of biotite, ^{40}Ar produced from radioactive decay of ^{40}K, may diffuse efficiently at temperatures above ~300°C (McDougall, Harrison, 1999). The date from Table 1 obtained from specific rocks (*e.g.*, diabase or lamprophyre) represent the cooling age of the dykes and closely correspond to the actual crystallization age of these rocks. The ^{40}Ar/^{39}Ar thermochronometry is the most common method, where obtained data are interpreted as crystallization ages for such specific magmatic systems (Kelley, 2002 and references therein).

The diabase dykes and other magmatic rocks within Kielce were formed during at least two main events (Table 1), in time frame that include Late Caledonian to Late Variscan tectonic regimes in the HCM. The individual ^{40}Ar/^{39}Ar ages obtained from Zalesie and Prągowiec diabases fall between 424 ±6 Ma and 254 ±12 Ma, respectively (Nawrocki *et al.*, 2007; Migaszewski, 2002). These oldest results were not undisputed, nevertheless, they point to Silurian age for the Zalesie diabase (part of Bardo intrusion). The youngest K-Ar data from Kielce Region are more dispersed. They range from 322 ±11 Ma (Podkranów lamprophyre) to 275 ±11 Ma (Wszachów lamprophyre), suggesting "a long-lasting and multiphasic formation of diabases and lamprophyres" in the HCM with its maximum activity in the Variscan (and post-Variscan?) time (Migaszewski, 2002).

This time span seems to be coeval with an emplacement of the silicic igneous rocks of the Małopolska Block, which are abundant at its southern margin. Their late Paleozoic age has been long, imprecisely referred, but using U-Pb SHRIMP II analyses of zircons from granitic rocks and their volcanic equivalents the time of igneous activity has been better constrained (Żelaźniewicz *et al.*, 2008). A new data set clearly highlights the events in Małopolska Block at 300 ±3 Ma (*op. cit.*) as well as at 305.2 ±1.5 Ma and at 292 ±4.5 Ma (Mikulski *et al.*, 2016).

U-Pb METHODOLOGY

Zircon grains from the lamprophyre, diabase and tuff rock-samples were separated at the University of Wrocław. A very small amount of grains was obtained from lamprophyre and diabase. Only a tuff sample contained the appro-

priate amount of grains. For dating purposes, only about 20 grains (Janowice-2) and about 30 grains (Podkranów), and more than two hundred zircon crystals from the tuff were hand-picked. They were placed in parallel rows on adhesive tape, and mounted in an epoxy resin disc together with chips of the standard Temora-2 zircon (^{206}Pb/^{238}U age of 416.8 ±0.3 Ma: Black *et al.*, 2004) and 91500 zircon as a reference for U-content (U = 78 ppm, a ^{207}Pb/^{206}Pb age of 1065.4 ±0.3 Ma, Wiedenbeck *et al.*, 1995). The mount surface was polished until the zircons had been sectioned exposing their internal microstructure. Subsequently, the grains were photographed under both transmitted light (TL) and reflected light (RL) mode using a Nikon Eclipse LU100NPol polarizing microscope. Scanning Electron Microscope (SEM) images of zircons and thin sections in this study were taken, using a HITACHI SU 3500 at the Polish Geological Institute – National Research Institute (PGI-NRI). The backscattered (BSE) images were used to control the quality of grains, and to select prismatic, acicular, euhedral zircon population (Fig. 2A–F). Internal morphologies have been investigated by SEM cathodoluminescence (CL) and they have been used as a guide for the selection of potential antecrysts or xenocrysts when present.

All U-Pb isotopic results reported here were collected on the SHRIMP IIe/MC instrument using a duoplasmatron as primary ions source. The isotopic ratios were analyzed using a *c.* 20–23 μm-diameter primary beam of ionized oxygen molecules $(O_2)^{1-}$ purified by a Wien filter. Before each analysis, the surface of the analysis site was cleaned by rastering of the primary beam for 2 min, in order to reduce the amount of common Pb on the mount surface. Secondary ions were collected on a single electron multiplier by cycling the magnet through five scans across the nine mass range of interest: ^{196}Zr$_2$O, ^{204}Pb, 204.1 (as a background), ^{206}Pb, ^{207}Pb, ^{208}Pb, ^{238}U, ^{248}ThO, and ^{254}UO. The analyses were collected in a sequence consisting of one analysis of a Temora-2 reference zircon measurement after every fourth unknown sample analysis, thus a single measurement of Temora-2 was made approximately every 1 hour during all analytical cycles.

SHRIMP U-Pb data were processed using open source SQUID-2 software (Ludwig, 2009) and plotted using Isoplot 3 (Ludwig, 2003) geochronological toolkits for Microsoft Excel. Common-Pb corrections for unknown samples were based on measured ^{204}Pb. The isotopic composition was calculated using the Pb isotopic evolution model of Stacey and Kramers (1975). The ages are ^{206}Pb/^{238}U for zircon grains <1000 Ma, and ^{207}Pb/^{206}Pb for those >1000 Ma, as a consequence of the relatively short half-life of the ^{235}U parent, making ^{207}Pb/^{206}Pb ages less precise than ^{206}Pb/^{238}U ages for relatively young zircons (Black *et al.*, 2004). The analytical results are listed in Table 2. The errors in data tables are 1σ, whereas weighted mean ages of individual samples are quoted at 2σ. The measurements were realized during three analytical sessions. The analyses of the reference zircon (Temora-2) over a longest session yielded a mean ^{206}Pb/^{238}U age of 416.8 ±2.6 Ma, 95% conf., MSWD = 0.58, n = 18 (giving a ^{206}Pb/^{238}U–^{207}Pb/^{235}U concordia age at 416.4 ±6.0 Ma), that was comparable to reference value of 416.78 ±0.33 Ma obtained on TIMS (Black *et al.*, 2004).

SAMPLE DESCRIPTION

The sample locations are shown in Figure 1, and briefly described individually in this chapter.

Kielce. The tuff sample was taken from lower part of the upper Silurian greywacke succession (about 140 m thick) of the Kielce Beds in the area of the Kielce Combined Power Plant, that contains a 10 cm thick layer of tuff (Malec, 2001). This coarse-grained pyroclastic rock was partially altered. The mineral assemblage includes: K-feldspar and plagioclase, quartz, biotite, with concentrations of fine-grained anatase, forming distinct bands, apatite, Fe-Ti oxides, and abundant zircon and monazite grains (Fig. 2G). This assemblage is accompanied by vitric clasts (>500 μm), with an advanced degree of devitrification. The glass shards are mostly replaced by zeolite.

Podkranów. The lamprophyre sample comes from a historical excavation of the Podkranów test pit (Rubinowski, 1962). The sample selected is from a relatively low in alteration, representing a "spherulitized" and coarse-grained intrusion (Kardymowicz, 1967). It contains curved phenocrysts of

→

Fig. 2. Backscattered electron (BSE) images of zircon grains extracted for U-Pb geochronology, taken at the magnification of ×500 and their host rocks

A, B – the auto- and antecrysts population with elongated, prismatic crystals in Kielce tuff; **C, D** – the xenocrysts selected from Podkranów lamprophyre with very rare elongated zircons and small subhedral grains; **E, F** – the xenocrystic grains from Janowice diabase dyke. A pit on zircon as seen in (BSE) image produced after SHRIMP analysis and rastered surface and a number of analysis is also shown; **G** – vitriclastic texture of partially altered tuff from Kielce, with abundant zircon (here euhedral and subrounded) as well as broken monazite grain; **H** – altered lamprophyre from Podkranów, containing zoned biotite, Fe-Ti oxides and apatite. Zircon grains are rare. Abbreviations: zrn – zircon, mnz – monazite, bt – biotite, ant – anatase, Fe-Ti ox – Fe-Ti oxide, cal – calcite, vitr – vitric clasts

Obrazy elektronów wstecznie rozproszonych (BSE) ziaren cyrkonu wybranych do badań geochronologicznych, wykonane przy powiększeniu ×500, oraz ich skał macierzystych

A, B – populacje auto- i antekryształów z wydłużonymi i pryzmatycznymi kryształami w tufie z Kielc; **C, D** – wybrane ksenokryształy cyrkonu z lamprofiru z Podkranowa z nielicznymi ziarnami wydłużonymi i małymi ziarnami subhedralnymi; **E, F** – ksenokryształy z dajki diabazu z Janowic. Widoczne owalne ślady po analizie w SHRIMP oraz numery analiz; **G** – tekstura witroklastyczna częściowo zmienionego tufu z Kielc z licznymi ziarnami cyrkonu (tu: euhedralne i półobtoczone) i spękanym ziarnem monacytu; **H** – wtórnie zmieniony lamprofir z Podkranowa zawierający pasowy biotyt, tlenki Fe-Ti i apatyt. Ziarna cyrkonu są nieliczne. Skróty: zrn – cyrkon, mnz – monacyt, bt – biotyt, ant – anataz, Fe-Ti ox – tlenek Fe-Ti, cal – kalcyt, vitr – szkliwo
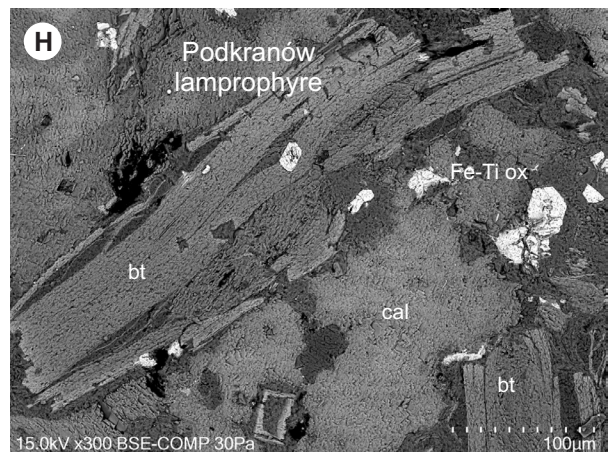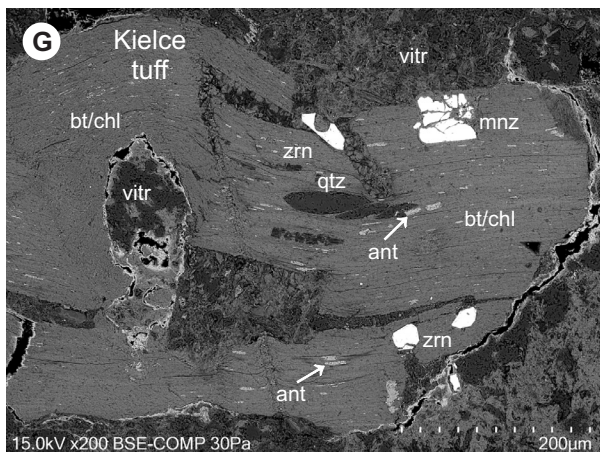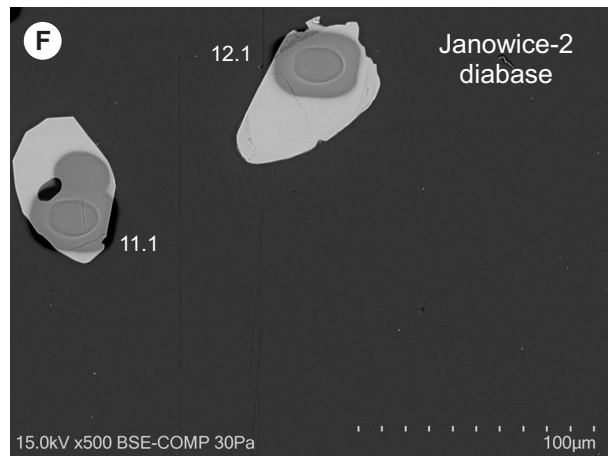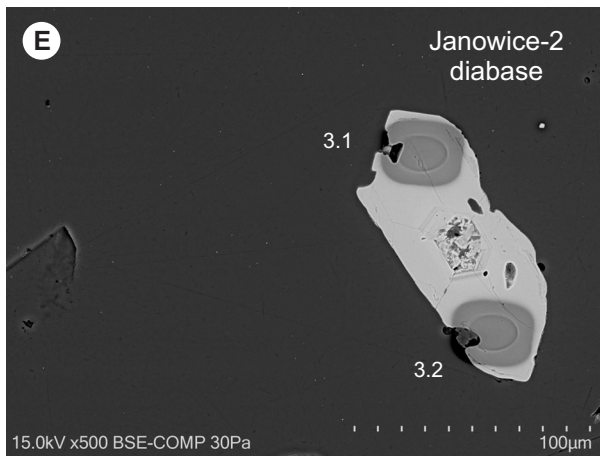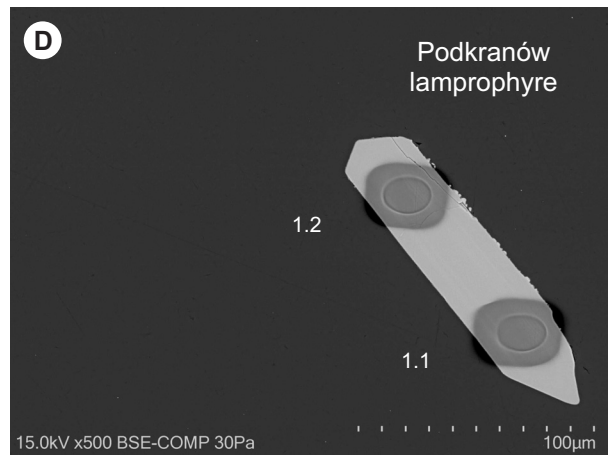
T a b l e 2

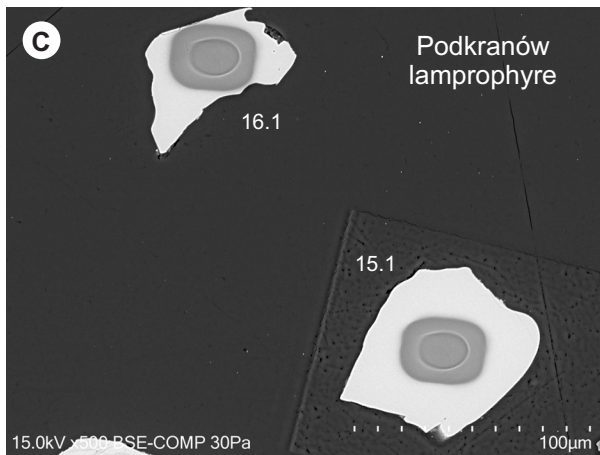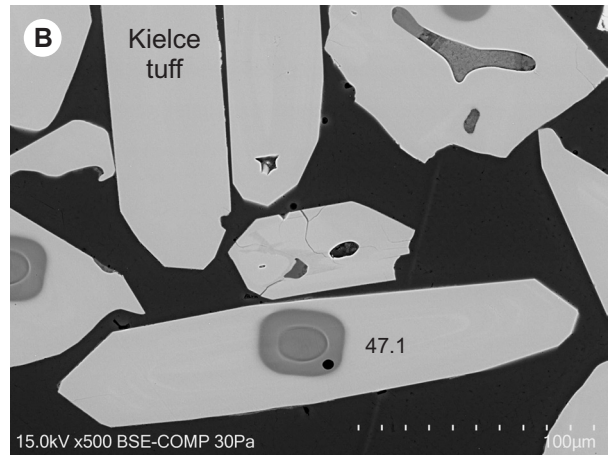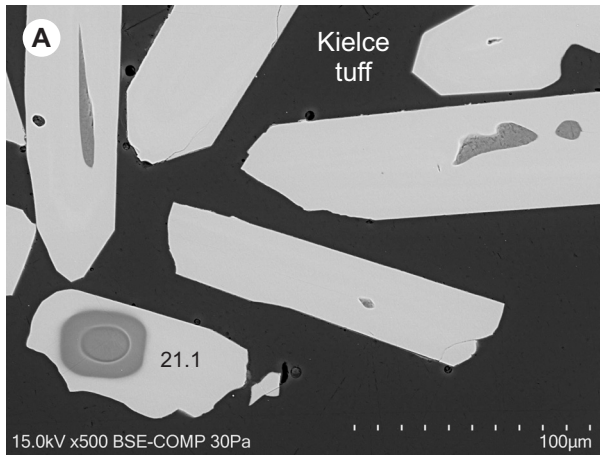**Zircon U-Pb isotopic data for the Kielce tuff, Podkranów lamprophyre and Janowice-2 diabase**

Dane izotopowe U-Pb dla cyrkonu z tufu z Kielc, lamprofiru z Podkranowa i diabazu z Janowic-2

Grain. spot	$^{206}Pb_c$ %	U ppm	Th ppm	$^{206}Pb^*$ ppm	$^{232}Th/^{238}U$	±%	$^{238}U/^{206}Pb^*$	±%	$^{207}Pb^*/^{206}Pb^*$	±%	$^{207}Pb^*/^{235}U$	±%	Age [Ma]	±
Kielce													$^{206}Pb/^{238}U$	
17.1	0.19	60	40	3.4	0.69	0.47	15.21	1.0	0.055	4.1	0.50	4.2	410	4
23.1	--	99	33	5.6	0.34	3.67	15.18	2.1	0.059	3.5	0.54	4.1	411	8
20.1	--	130	111	7.4	0.88	1.21	15.08	0.8	0.064	4.1	0.58	4.1	414	3
19.1	--	133	11	7.6	0.09	1.40	15.02	0.7	0.059	2.2	0.54	2.3	415	3
47.1	--	106	78	78	0.76	1.94	15.15	1.4	0.071	5.3	0.65	5.5	412	6
81.1	--	72	39	39	0.56	0.80	15.14	1.5	0.069	6.4	0.62	6.5	412	6
62.1	1.53	68	31	31	0.47	0.68	15.10	1.5	0.042	10.6	0.38	10.7	413	6
82.1	1.98	84	53	53	0.65	2.31	15.09	1.5	0.039	12.5	0.36	12.6	414	6
77.1	0.78	249	256	256	1.06	0.59	15.09	1.3	0.049	4.3	0.45	4.5	414	5
56.1	--	35	50	50	1.50	0.86	15.03	1.7	0.055	8.0	0.50	8.2	415	7
57.1	--	110	33	33	0.31	3.88	15.03	1.3	0.056	3.0	0.51	3.2	415	5
76.1	0.53	70	51	51	0.76	0.71	15.00	1.4	0.052	5.9	0.48	6.1	416	6
53.1	--	99	11	11	0.11	2.75	15.00	1.3	0.065	4.0	0.60	4.2	416	5
61.1	1.49	108	41	41	0.39	1.31	14.98	1.4	0.042	8.4	0.39	8.5	417	5
58.1	2.63	55	16	16	0.29	2.12	14.97	1.6	0.035	19.9	0.33	20.0	417	6
74.1	3.35	25	12	12	0.50	0.92	14.88	2.2	0.029	39.8	0.27	39.9	419	9
77.2	0.55	93	20	20	0.22	0.65	14.83	1.4	0.053	6.7	0.50	6.8	421	6
67.1	--	103	85	85	0.86	0.66	14.79	1.4	0.068	6.0	0.64	6.2	422	6
75.1	--	147	146	146	1.03	0.61	14.79	1.3	0.061	4.4	0.57	4.6	422	5
59.1	0.48	256	154	154	0.62	1.69	14.73	1.2	0.052	2.7	0.49	2.9	424	5
54.1	--	92	9	9	0.10	0.62	14.66	1.3	0.061	2.7	0.58	3.0	425	5
66.1	--	66	22	22	0.35	2.32	14.62	1.5	0.067	6.8	0.63	7.0	426	6
49.1	1.04	82	57	57	0.71	0.66	14.58	1.4	0.046	7.7	0.44	7.8	428	6
50.1	1.28	132	62	62	0.48	1.27	14.57	1.3	0.045	6.1	0.42	6.2	428	5
80.1	0.64	117	113	113	1.00	0.65	14.48	1.4	0.050	5.5	0.48	5.7	430	6
71.1	0.80	58	28	28	0.49	0.74	14.47	1.5	0.050	7.8	0.47	7.9	431	6
60.1	--	80	17	17	0.22	0.65	14.43	1.4	0.068	5.4	0.65	5.6	432	6
51.1	--	66	29	29	0.46	0.69	14.39	1.4	0.064	5.6	0.62	5.8	433	6
72.1	--	68	20	20	0.31	0.69	14.37	1.5	0.068	6.0	0.65	6.2	434	6
78.1	--	79	18	18	0.24	1.76	14.36	1.5	0.068	6.3	0.66	6.5	434	6
55.1	0.54	82	44	44	0.56	0.75	14.35	1.4	0.050	5.4	0.48	5.6	434	6
63.1	--	125	80	80	0.66	0.61	14.32	1.3	0.057	3.1	0.55	3.4	435	5
84.1	--	123	36	36	0.30	0.63	14.26	1.4	0.065	4.3	0.63	4.5	437	6
68.1		77	19	19	0.26	0.67	14.00	1.5	0.077	6.9	0.76	7.1	445	6
xenocrysts														
14.1	--	194	35	13.9	0.19	2.29	12.30	2.7	0.0560	2.5	0.628	3.2	504	13
39.1	--	69	19	5.2	0.28	0.43	10.82	3.0	0.0629	2.8	0.801	3.7	570	16
37.1	--	118	75	9.8	0.66	0.35	10.40	3.1	0.0544	4.2	0.721	4.9	592	17
8.1	--	49	21	4.5	0.44	0.62	9.71	3.7	0.0596	4.3	0.847	5.2	632	22
													$^{207}Pb/^{206}Pb$	
4.1	--	116	32	15.7	0.28	0.61	6.38	1.8	0.105	6.0	2.26	6.2	1712	110
86.1	8.82	205	64	39.3	0.32	0.80	4.21	3.3	0.120	3.0	3.80	3.6	1950	67
1.1	--	65	47	19.0	0.74	0.71	2.92	1.5	0.125	4.2	5.90	4.4	2028	74
Podkranów													$^{206}Pb/^{238}U$	
20.1	--	461	202	19.4	0.45	0.66	20.1	3.5	0.056	2.2	0.4	3.6	313	11
4.1	--	348	88	15.2	0.26	0.20	19.5	3.4	0.055	1.8	0.4	3.5	322	11
10.1	--	189	37	8.4	0.20	0.25	19.5	3.4	0.052	2.3	0.4	3.8	322	11
xenocrysts														
1.1	--	113	64	6.2	0.58	1.08	15.6	3.2	0.064	3.3	0.6	4.2	400	13
1.2	--	74	39	4.1	0.54	0.44	15.4	3.9	0.056	5.1	0.5	5.9	406	16
12.1	--	69	17	3.8	0.25	1.62	15.6	4.0	0.052	4.9	0.5	5.8	402	16
5.1	--	114	60	6.4	0.54	0.83	15.6	3.8	0.058	3.6	0.5	4.8	400	15
14.1	--	152	258	11.7	1.75	0.32	11.7	5.2	0.066	25.7	0.8	27.8	522	17
27.1	--	51	47	4.1	0.95	0.56	10.3	3.9	0.069	4.3	0.9	5.5	588	19
11.1	--	129	93	10.7	0.75	0.97	12.1	4.9	0.057	15.9	0.6	17.5	512	20
17.1	--	719	17	100.5	0.02	2.18	6.0	3.2	0.095	0.5	2.2	3.1	962	29

Table 2 cont.

Grain. spot	$^{206}Pb_c$ %	U ppm	Th ppm	$^{206}Pb^*$ ppm	$^{232}Th/^{238}U$	±%	$^{238}U/^{206}Pb^*$	±%	$^{207}Pb^*/^{206}Pb^*$	±%	$^{207}Pb^*/^{235}U$	±%	Age [Ma]	±
xenocrysts													$^{207}Pb/^{206}Pb$	
17.1	--	719	17	100.5	0.02	2.18	6.0	3.2	0.095	0.5	2.2	3.1	1533	9
23.1	--	100	28	14.6	0.29	0.36	6.2	3.6	0.074	1.6	1.7	3.6	1035	33
15.1	--	131	37	19.4	0.30	0.32	5.7	3.5	0.075	1.4	1.8	3.4	1073	29
8.1	--	34	25	5.2	0.76	0.70	5.6	4.9	0.075	5.1	1.8	6.5	1078	102
6.1	--	157	9	31.8	0.06	1.50	4.1	3.3	0.090	0.7	3.0	3.3	1434	14
24.1	--	88	21	19.3	0.25	0.37	3.9	3.6	0.095	1.1	3.4	3.5	1534	21
21.1	--	71	15	17.1	0.21	1.22	3.5	3.2	0.107	0.4	4.2	3.2	1741	8
18.1	--	382	25	95.5	0.07	0.20	3.4	3.9	0.109	1.6	4.4	3.6	1775	29
9.1	--	98	51	25.0	0.54	0.40	3.4	3.7	0.111	1.1	4.5	3.6	1813	20
26.1	--	88	30	23.2	0.35	0.37	3.3	3.7	0.109	1.1	4.5	3.4	1786	21
25.1	--	79	53	23.7	0.69	0.42	2.7	3.9	0.124	1.7	6.2	3.5	2017	30
19.1	--	56	38	17.3	0.70	0.54	2.7	3.4	0.131	1.8	6.6	3.2	2106	32
16.1	--	73	23	29.4	0.32	0.43	2.1	3.7	0.176	1.7	11.7	3.5	2618	28
3.1	--	115	66	49.9	0.59	0.33	2.0	3.8	0.192	1.0	13.2	3.3	2760	16
Janowice-2													$^{206}Pb/^{238}U$	
7.1	--	170	80	7.1	0.63	1.4	21.0	3.4	0.0539	4.5	0.35	5.1	300	10
xenocrysts														
2.1	--	78	18	4.3	0.32	1.7	15.9	3.5	0.0571	3.4	0.50	4.5	393	14
8.1	--	144	12	7.9	0.28	1.5	15.7	3.2	0.0549	3.4	0.48	4.0	399	12
6.1	--	124	116	6.8	0.61	1.4	15.4	3.3	0.0631	2.6	0.56	3.8	405	13
4.1	--	97	20	5.4	1.32	1.5	15.5	3.9	0.0656	7.9	0.58	9.3	402	15
10.1	--	72	40	4.0	0.12	1.3	15.9	3.0	0.0589	2.3	0.51	3.5	393	11
13.1	--	48	24	2.7	1.05	1.7	14.4	3.9	0.0621	7.5	0.60	8.7	434	16
8.2	--	76	46	4.4	0.75	1.7	14.8	2.2	0.0567	4.9	0.53	5.5	420	9
11.1	--	179	79	10.3	0.65	1.8	15.1	3.7	0.0548	5.3	0.50	6.1	414	15
4.2	--	56	44	3.2	0.81	1.7	15.1	3.8	0.0640	5.0	0.58	6.0	413	15
3.2	--	167	27	10.7	0.21	1.5	13.9	3.3	0.0483	3.1	0.48	4.2	447	14
1.1	1.52	199	27	14.5	0.20	4.2	12.1	3.2	0.0691	4.3	0.79	5.1	512	16
3.1	1.83	128	39	9.9	0.40	1.6	11.2	3.5	0.0623	2.8	0.77	4.0	552	18
xenocrysts													$^{207}Pb/^{206}Pb$	
5.1	--	303	57	61.8	0.25	1.3	4.3	3.0	0.1006	0.8	3.20	3.0	1634	15
9.1	--	148	85	34.6	0.74	1.5	3.7	3.4	0.0979	2.3	3.64	3.5	1585	42
12.1	--	158	37	46.2	0.31	1.3	3.0	3.0	0.1194	0.8	5.48	2.8	1948	14

Errors are 1-sigma; Pb_c and Pb^* indicate the common and radiogenic portions, respectively. Common Pb corrected using measured ^{204}Pb. Error in standard calibration was 0.32% for Kielce, 0.89% for Podkranów, and 0.28% for Janowice-2 sample

Błędy oznaczenia na poziomie 1 sigma; Pb_c and Pb^* oznaczają odpowiednio: ołów zwyczajny i ołów radiogeniczny. Pb zwyczajny skorygowany za pomocą zmierzonej ^{204}Pb. Błąd kalibracji wzorca wyniósł 0,32% dla próbki z Kielc, 0,89% dla Podkranowa i 0,28% dla próbki z Janowic-2

biotite, shown using BSE a regular zoning with a high-Mg core and Fe-rich rims (Fig. 2H), including apatite, Fe- oxides enclosed in a fine-grained matrix, dominated by secondary calcite.

Janowice-2. The sample of diabase from a few mafic dykes intruding the Łysogóry Region, split into two segments, *i.e.*, the Milejowice (southern) and Janowice (northern). Their petrographic features were summarized by Kowalczewski (2004), and complemented by geochemistry and petrographic recognition (Krzemiński, 2004). The rock selected from Janowice consist mainly of plagioclase and pyroxene, represented by augite (diopside). Subordinate minerals are biotite flakes and needle-shaped apatite; amphibole and Fe- and Ti-oxides, but zircon grains are rare, due to low contents of Zr (whole-rock analyses about 100 ppm Zr).

U-Pb RESULTS AND THEIR INTERPRETATION

The samples from the lamprophyre, diabase and tuff layer referred in this contribution contain variable amounts of volcanic and older inherited zircon grains, and a mixed population of pyroclastic zircons. Typically for pyroclastic zircons, the most statistically robust method to evaluate the maximum magmatic age (or deposition age) is the weighted mean of the youngest cluster of three or more single-grain dates that overlap within 2σ uncertainty (Dickinson and Gehrels, 2009; McKay *et al.*, 2015). The $^{238}U/^{206}Pb$ is the most appropriate decay chain to analyze for volcanic rocks older than 150 Ka due to the accurately measurable quantity of ^{206}Pb present by that age (Hanchar and Watson, 2003). In this study a concordia age for youngest and other prominent clusters has also been calculated.

Kielce. The Kielce tuff sample is dominated by relatively monotonous population of large well-formed elongate, euhedral zircons typical of primary volcanic-derived crystals, with a small amount of subrounded xenocrysts. Abundant fluid inclusions are noted (Fig. 2A, B). Cathodoluminescence images (CL) expose uniform zoning typified by oscillatory zones that parallel the long dimension of the grains (Fig. 3B). Excluding rare xenocrysts, the needle-like habit of volcanogenic zircon produced a range of $^{206}Pb/^{238}U$ ages from 437 ±6 Ma to 410 ±4 Ma (Table 2). This extended age range (*c.* 27 Ma) could be due to commonly recycled older zircon into later volcanic events (Miller *et al.*, 2007). These results form three clusters peaked at *ca.* 432, *ca.* 425, and *ca.* 414.5 Ma (Fig. 3A) and they plot on or close Tera–Wasserburg concordia curve. A younger cluster of analyses

(n = 9), with a youngest concordant grain with $^{206}Pb/^{238}U$ age of 410 ±4 Ma versus $^{207}Pb/^{206}Pb$ age of 422 ±91 Ma (=3% disc) accompanies a few grains in the range of 412–414 Ma.

The calculation based upon these four most precise results (percentage of discordance between 5 and 7) yields an Early Devonian concordia age at 414.2 ±6.6 Ma (Fig. 3D). This age is interpreted as the best estimate of the maximum magmatic age for Kielce tuff horizon, but the numerous zircon grains, most probably represent an antecrysts population, that was incorporated from material left from an older episode of magmatic activity in Silurian about 425–424 Ma. For this dominant group of grains the weighted average $^{206}Pb/^{238}U$ age was calculated at 425.4 ±3 Ma (MSWD = 1.6, n = 24). The Tera–Wasserburg (T-W) and Wetherill (W) concordia diagrams constrained for these antecrysts yielded

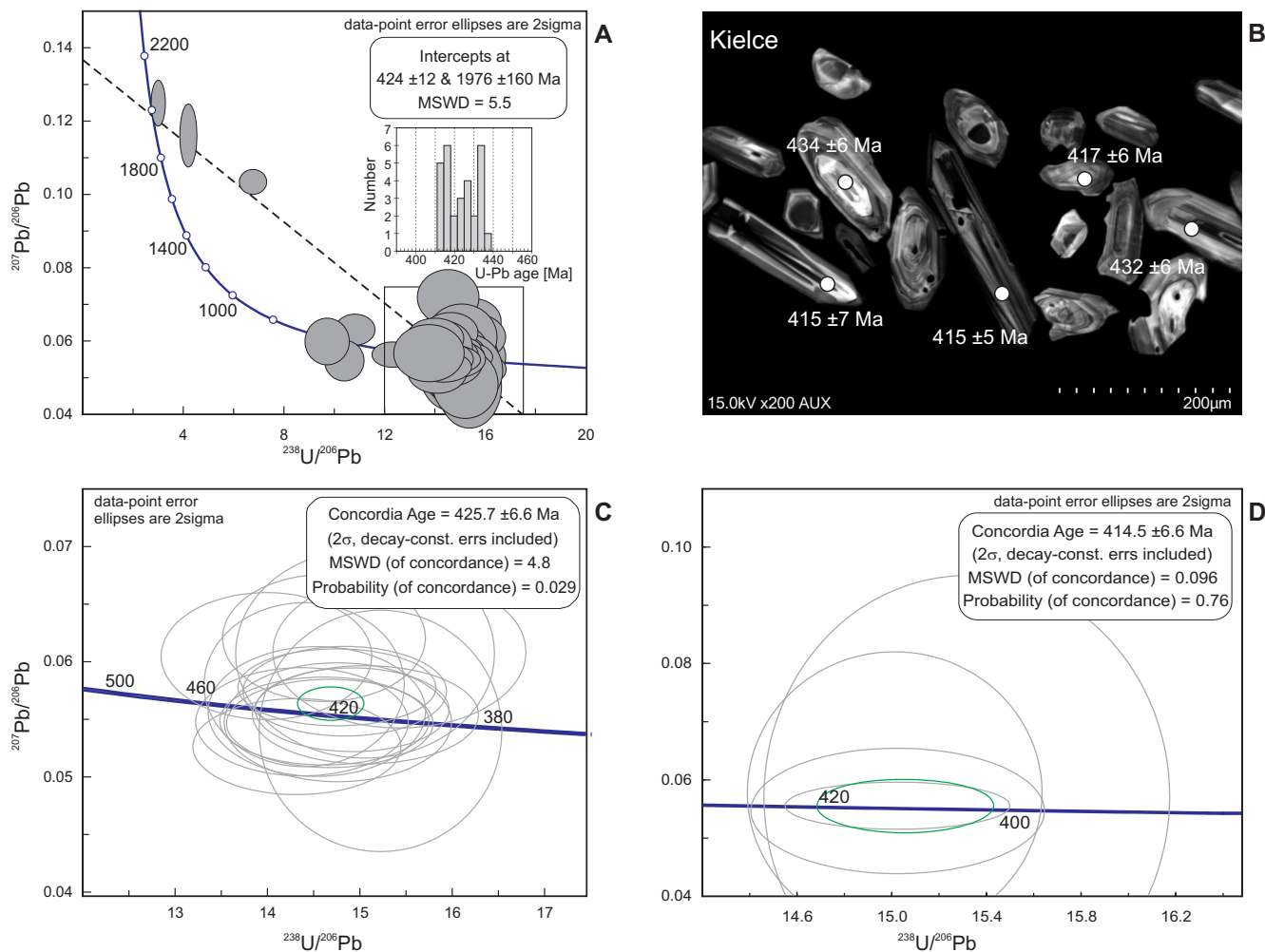**Fig. 3. A. Concordia diagram for all analyzed zircon grains from Kielce tuff with detected populations of xenocrysts, antecrysts and autocrysts. B. Catholuminescence image of a zircon grains showing location of SHRIMP II/MC spots with $^{206}Pb/^{238}U$ ages. C. Concordia diagram for antecrysts. D. Concordia diagram for autocrysts estimating the maximum eruption age at 414.5 ±6.6 Ma (earliest Devonian: Lochkovian)**

A. Diagram konkordii dla wszystkich analizowanych ziaren cyrkonu z tufu z Kielc z populacją ksenokryształów, antekryształów i autokryształów. **B.** Obraz katodoluminescencyjny wybranych ziaren z lokalizacją analiz SHRIMPII/MC i wiekiem $^{206}Pb/^{238}U$. **C.** Diagram konkordii dla antekryształów. **D.** Diagram konkordii dla autokryształów określający maksymalny wiek erupcji 414,5 ±6,6 mln lat (wczesny dewon: lochkow)

a similar age within error (Fig. 3C) at 425.7 ±6.6 Ma (MSWD = 4.8) and at 423.8 ±3.9 Ma (MSWD = 0.004) respectively. Thus the age results revealed a mixed volcanogenic zircon population within one stratigraphic layer of the pyroclastic horizon. (Fig. 3A).There is also anomalously older, pre-Silurian group of grains, so-called xenocrysts. They document an Ediacaran concordia age of 594 ±20 Ma (n = 3, MSWD = 0.0024) and probably Paleoproterozoic single grains *e.g.* ^{207}Pb/^{206}Pb ages of *ca.* 2028, *ca.* 1950, and *ca.* 1712 Ma. This last group is poorly preserved, contaminated by common lead and discordant.

Podkranów. The sample from Podkranów lamprophyre reveals a complex zircon grains collection. The grain morphologies range from elongate sharp prisms to sub- and well-rounded grains (Fig. 2C, D). The U-Pb analysis gave strongly dispersed age distributions (Fig. 4A), caused by abundant xenocrysts. The oldest population consists of two Archean grains (^{207}Pb/^{206}Pb ages of *ca.* 2760 and *ca.* 2618 Ma) and twelve Proterozoic (^{207}Pb/^{206}Pb ages from *ca.* 2106 to *ca.* 1035 Ma) as well as one discordant zircon. There is also a group of Cambrian grains with age between *ca.* 522 and *ca.* 512 Ma. The next group is represented by four early Devonian grains with ^{206}Pb/^{238}U ages between 406 ±16 Ma and 400 ±15 Ma. They yielded (Fig. 4C) a weighted average ^{206}Pb/^{238}U age at 402 ±14 Ma (n = 4, MSWD = 0.036) and concordia age at 403 ±18 Ma (MSWD = 0.23). These xenocrysts were incorporated from the surrounding host rocks during emplacement of the lamprophyric magma. The youngest population (Fig. 4D) consists of three Carboniferous grains in range from 322 ±11 to 313 ±11 Ma, yielding a con-
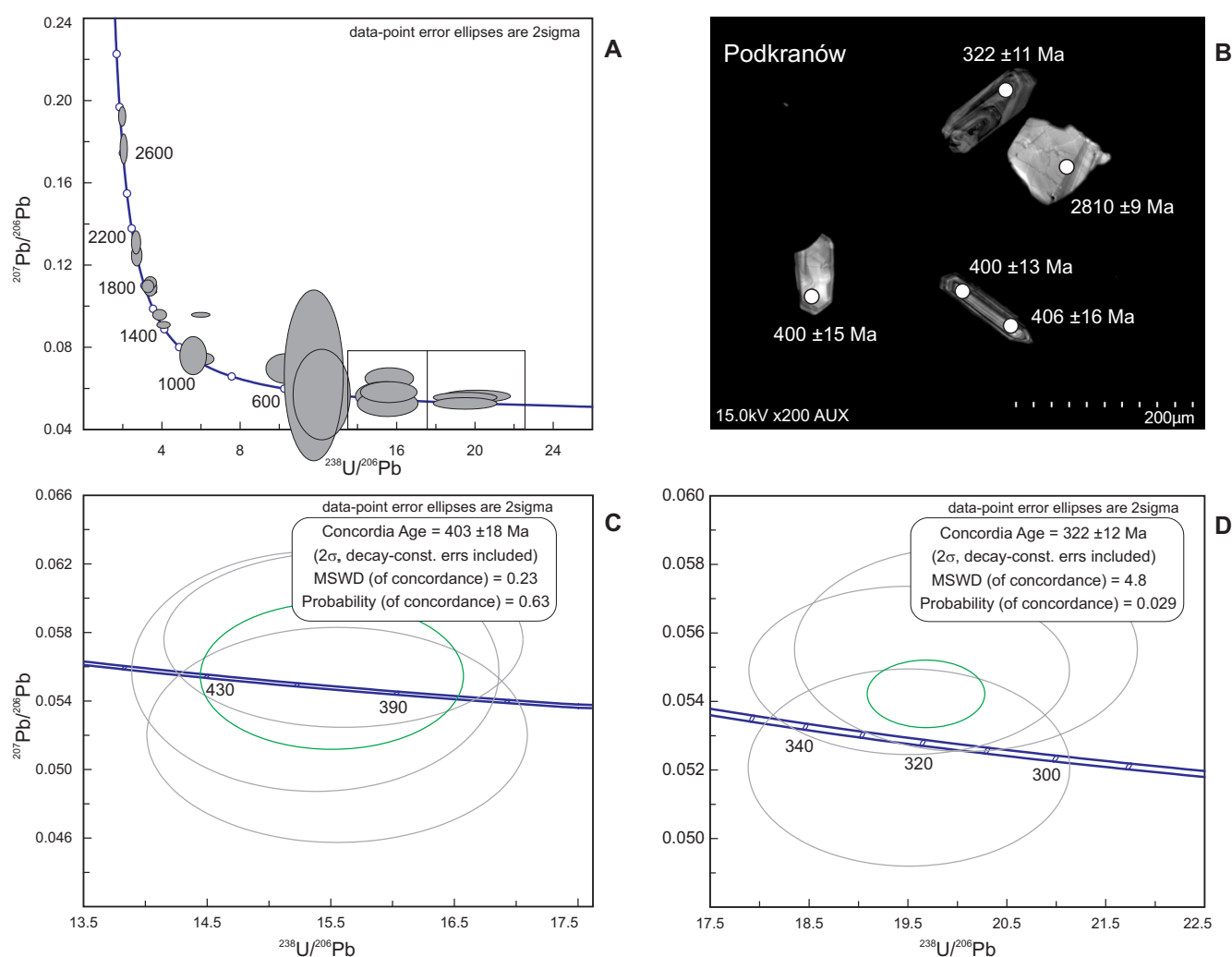

Fig. 4. A. Concordia diagram for all analyzed zircon grains from Podkranów lamprophyre with a predominant group of xenocrysts, as well as antecrysts and autocrysts. **B.** Catholuminescence image of selected zircon grains showing location of SHRIMP II/MC spots with ^{206}Pb/^{238}U ages and ^{207}Pb/^{206}Pb ages (>1 Ga). **C.** Concordia diagram for antecrysts. **D.** Concordia diagram for youngest autocryst estimating the emplacement age at 322 ±12 Ma (Early Pennsylvanian: Bashkirian)

A. Diagram konkordii dla wszystkich analizowanych ziaren cyrkonu z lamprofiru z Podkranowa z dominującą grupą ksenokryształów, antekryształami i autokryształami. **B.** Obraz katodoluminescencyjny wybranych ziaren pokazujący lokalizację analizowanych punktów i wiek ^{206}Pb/^{238}U oraz ^{207}Pb/^{206}Pb (dla >1 mld lat). **C.** Diagram konkordii dla antekryształów. **D.** Diagram konkordii dla najmłodszego autokryształu z wiekiem posadowienia 322 ±12 mln lat (wczesny pensylwan: baszkir)

cordia age at 322 ±12 Ma (MSWD = 4.8), that is interpreted as the time closest to subvolcanic emplacement of Podkranów lamprophyre.

Janowice-2. The zircon grains selected from Janowice-2 diabase are sub- to well-rounded, and are fine-grained crystals (Fig. 2E, F), with some evidence of resorption. The CL images (Fig. 5B) show simple oscillatory zoning but a distinct type of pattern indicates an igneous origin but from different source rocks. The analysis were plotted on a concordia Tera–Wasserburg diagram (Fig. 5A), showing a several age groups. The oldest grain has a Paleoproterozoic $^{207}Pb/^{206}Pb$ age of 1948 ±14 Ma, accompanied with two Mesoproterozoic ages of *ca.* 1585 Ma and 1634 ±14 Ma as well as Ediacaran/Cambrian grains of 552 ±18 to 512 ±16 Ma. The dominant xenocrysts group gave nearly concordant late

Silurian ages with an upper intercept age at 418.3 ±9.7 Ma. The youngest age was determined on a single grain, providing a concordant result with a $^{206}Pb/^{238}U$ age of 300.1 ±10 Ma versus a $^{207}Pb/^{206}Pb$ age of 308 ±51 Ma (Fig. 5D). This one spot indicates a Carboniferous crystallization age.

DISCUSSION

All samples from the HCM dated herein reveal complex zircon populations, that document the intricate histories of growth accompanied by significant incorporation of older material. Tuff layers, or their weathered equivalents as well as mafic dykes (diabase and lamprophyre), are crucial geochronological marker horizons that may improve correlations
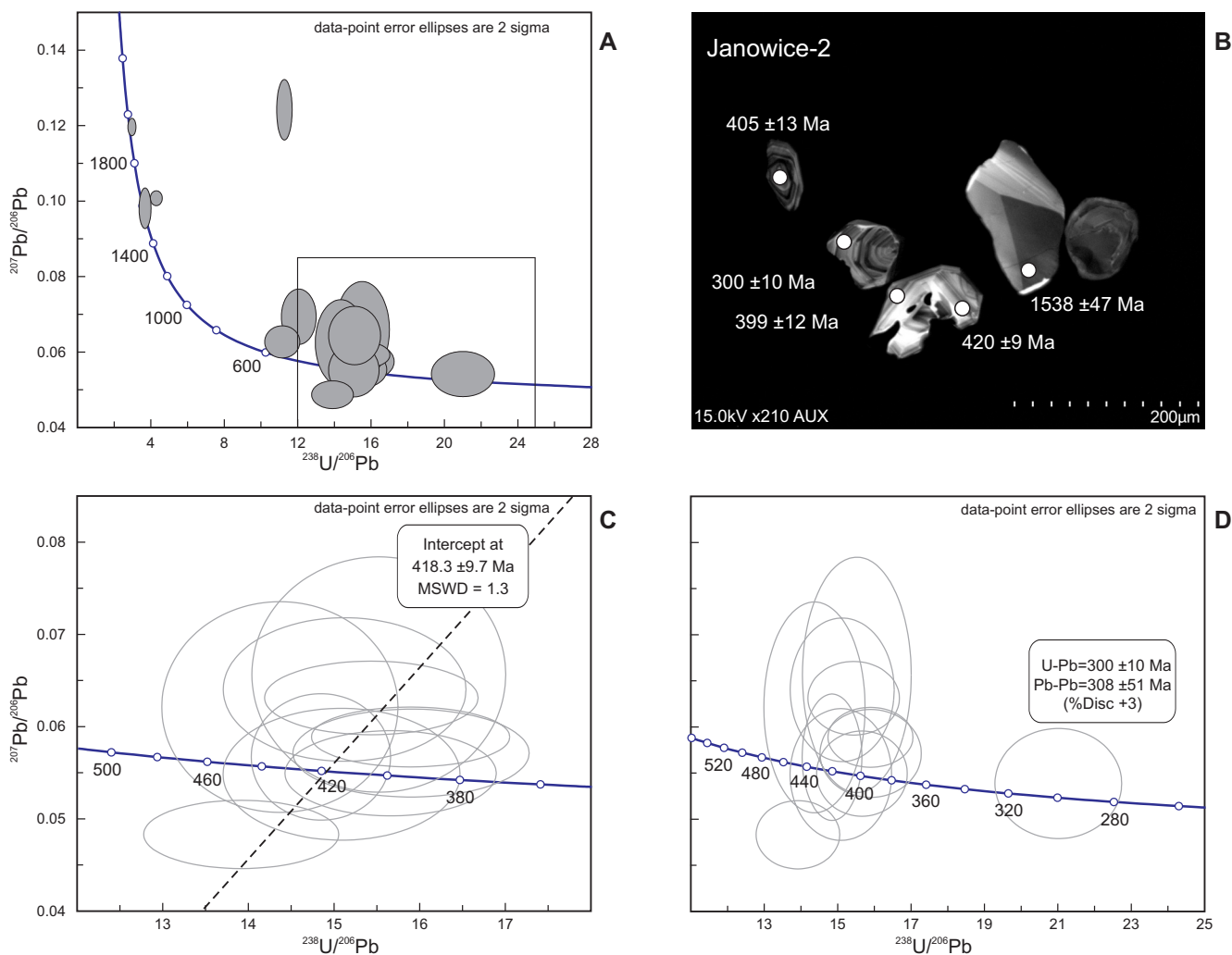

Fig. 5. A. Concordia diagram for zircon grains from Janowice-2 diabase with xenocrysts, antecrysts and only a few that can be directly related to intrusive veinlets. **B.** Catholuminescence image of zircon antecrysts, partially remelted, and the youngest grain; the location of SHRIMP II/MC spots are shown. **C.** Concordia diagram for antecrysts. **D.** Concordia diagram and age of youngest autocryst crystalized at 300 ±10 Ma (Late Pennsylvanian)

A. Diagram konkordii dla ziaren cyrkonu z diabazu z Janowic-2 z ksenokryształami, antekryształami i nielicznymi ziarnami, które mogą być bezpośrednio związane z intruzją. **B.** Obraz katodoluminescencyjny częściowo nadtopionych antekryształów oraz najmłodszych ziaren; pokazano lokalizację punktów analitycznych. **C.** Diagram konkordii dla wybranych antekryształów. **D.** Diagram konkordii dla najmłodszego autokryształu o wieku krystalizacji 300 ±10 mln lat (późny pensylwan)

and regional chronostratigraphy, therefore the radiometric dating of these horizons are mainly focused on deposition or emplacement age determination, using the youngest closed--system zircons from the non-reworked ash bed or dykes, which if grains are syn-magmatic autocrysts, should equal the eruption age of the tuff or emplacement of mafic dyke. The calculation of weighted mean age of the youngest cluster of three or more single-grain dates that overlap within 2σ uncertainty (Dickinson, Gehrels, 2009; McKay *et al.*, 2015) and is an effective and widely accepted strategy. During this study this strategy was completed by constraining the $^{206}Pb/^{238}U$ versus $^{207}Pb/^{206}Pb$ concordia ages (Table 3). In this context, for regional comparison these values are a more reliable approximation of the maximum eruption age.

Until the present contribution, there have been no isotopic ages published from the ~10 cm thick layer of tuff recognized (Malec, 2001) in the lower part of the greywacke succession in the Kielce Region. The youngest zircon cluster document early Devonian volcanic phase at 414.5 ±6.6 Ma. All obtained ages, including the concordia T-W, $^{206}Pb/^{238}U$ weighted average and youngest single grain are consistent. They well correspond to the Ar-Ar dates of Zarobiny (Fig. 1) diabase emplacement (Nawrocki *et al.*, 2013), which likely represent minimum (cooling) ages and are not influenced by "magma chamber inheritance" (Fig. 6B).

Moreover a coarse-grained tuff horizon in Kielce preserved a high concentration of large well-formed elongate, euhedral crystals (Fig. 2A, B), with uniform zoning parallel the long dimension of the grains, that crystallized at 425.7 ±6.6 Ma (concordia T-W). However this prominent population of antecrysts predates the eruption age significantly by at least 10 Ma. These grains were incorporated from material left from older episodes of magmatic activity at the same center indicating that zircon-saturated magma was present earlier in the history of this magmatic system. A high concentration of zircons in the ash bed, could be explained by the felsic chemistry of parental magma (high Zr element content >>100 ppm) and by the proximal character of deposit, where the heavier components of the ash cloud (*e.g.* large zircons) fell to the ground before the lighter components. The record of the pre-erupted history obtained from Kielce tuff seems to be coeval to emplacement of the Bardo dykes, with a diabase dated in Zalesie by Ar-Ar technique at

424 ±6.6 Ma (Nawrocki *et al.*, 2007). Such broadly coeval results (Fig. 6B) support the accuracy of the obtained age data. The magmatic ages for individual sites in the HCM, however, are slightly older than the $^{40}Ar/^{39}Ar$ cooling ages, and reflect differences of the close temperatures between U-Pb and Ar-Ar (K-Ar) systems. The U–Pb ages of 425.7 ±6.6 and 414.5 ±6.6 Ma reported from volcanic zircons in this pyroclastic horizon place robust temporal constraints on the timing of the prominent stage of magmatism in the Kielce Region. It was a most extensive magmatic activity of the HCM, and occurred mainly in the Bardo Syncline in central part of this region (Fig. 1), and was accompanied by an ash flow deposit exposed in Kielce. No sedimentary continuity is observed in the Kielce Region (Malec, 2001), subjected to stronger uplifting movements and tectonic activity at the Silurian/Devonian transition.

During the Silurian, the HCM was a part of the Caledonian foreland basin, that extended from Norway to Romania and Moldova. The prolonged collision between Baltica, and Avalonia with the major orogen-parallel, strike-slip motion along the Iapetus occurred between 425–410 Ma, and the final deformation event within the Caledonian foreland took place in the earliest Devonian (Mazur *et al.*, 2018 and references therein). These events are also synchronous with a number of upper Wenlock and lower Ludlow distal ash beds (K-bentonites) dispersed in many parts of Europe from the British Islands to Estonia–Latvia–Lithuania–Gotland (427.8 ±0.68 Ma) and HCM (Trela *et al.*, 2018 and references therein), to Podolia, which emphasize their significance in this region.

The next record of magmatic activity with ages of 322 ±12 and 300 ±10 Ma obtained from the Podkranów lamprophyre (Kielce Region) and Janowice diabase (Łysogóry Region) is related to the Late Variscan orogenic phase. During this time, I-type granites, porphyritic dacites and rhyolites were successively emplaced along the SW margin of the Małopolska Block (Żelaźniewicz *et al.*, 2008; Nawrocki *et al.*, 2013; Mikulski *et al.*, 2016). Their ages, revealed by U-Pb zircon study and Ar-Ar whole rock analyses were compared to the newly obtained age results from this study (Fig. 6A). The maximum magmatic ages constrained by youngest zircon grains or cluster from lamprophyre and diabase fit into the set of geochronological data compiled from

Summary of zircon U-Pb isotopic data for the Kielce tuff, Podkranów lamprophyre and Janowice-2 diabase

Podsumowanie wyników analiz U-Pb cyrkonu z tufu z Kielc, lamprofiru z Podkranowa i diabazu z Janowic-2

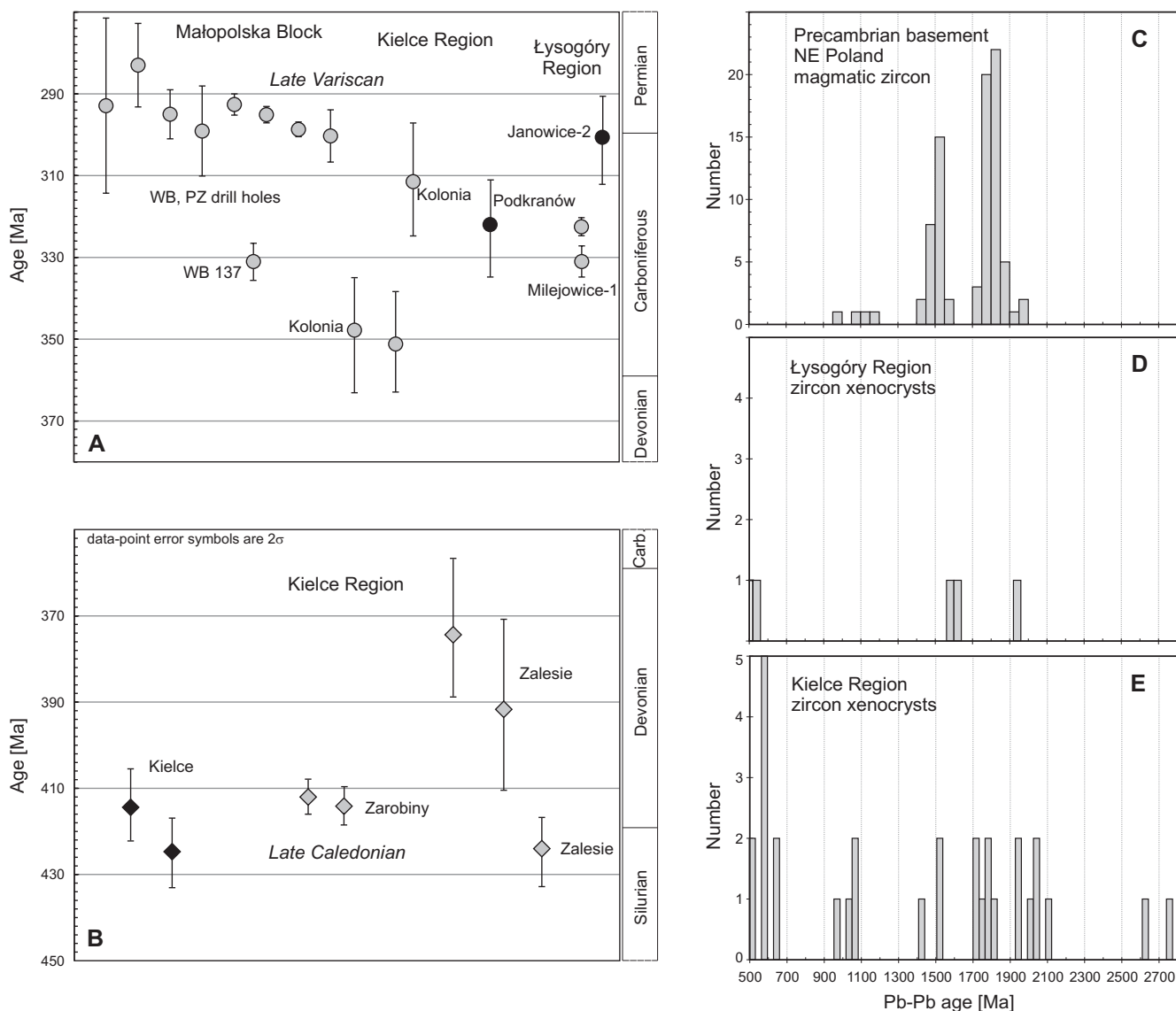| Sample	Region	Youngest grain [Ma]	Cluster	$^{206}Pb/^{238}U$ Weighted av. [Ma]	MSWD	n	Concordia T-W [Ma]	MSWD	n
Kielce tuff	KR	410 ±4	I	413 ±2.9	0.16	4	414.5 ±6.6	0.096	5
			II	425.4 ±3	1.6	24	425.7 ±6.6	4.8	24
Podkranów lamprophyre	KR	313.5 ±12	I	319.5 ±12	0.23	3	322 ±12	4.8	3
			II	402.4 ±14	0.036	3	403 ±18	0.23	3
Janowice-2 diabase	Ł	300 ±10	I	398 ±5.7	0.65	5			
			II	411.4 ±12	1.7	10	418.3 ±9.7	1.3	10

Fig. 6. Schematic diagrams summarizing Late Variscan (A) and Late Caledonian (B) magmatic events within the geologic time scale

Data obtained from the autocrysts and antecrysts (black marks: U-Pb concordia ages, this study) compared with the published dating results (gray marks) Data taken from: Ar-Ar and K-Ar cooling ages, HCM area – Migaszewski (2002); Nawrocki *et al.* (2007, 2013); U-Pb zircon ages from Małopolska Block – Żeláźniewicz *et al.* (2009); Nawrocki *et al.* (2010); Mikulski *et al.* (2016). Histograms comparing the Pb-Pb zircon data for: **C** – magmatic rocks recognized in Precambrian basement of NE Poland (data from Krzemińska *et al.*, 2017); **D** – xenocrysts population detected in Łysogóry Region (Janowice diabase); **E** – xenocrysts detected in Kielce Region (Kielce tuff and Podkranów lamprophyre)

Schematyczne diagramy podsumowujące waryscyjskie (A) i kaledońskie (B) zdarzenia magmowe wraz ze skalą czasu geologicznego

Dane uzyskane z autokryształów i antekryształów (czarne znaczniki: wieki konkordii U-Pb; niniejsza praca) porównane z publikowanymi wynikami datowania (szare znaczniki). Źródła danych: wiek stygnięcia K-Ar i Ar-Ar, obszar HCM – Migaszewski (2002); Nawrocki i in. (2007, 2013); wiek U-Pb cyrkonu z bloku małopolskiego – Żeláźniewicz i in. (2009); Nawrocki i in. (2010); Mikulski i in. (2016). Histogramy porównujące wiek Pb-Pb: **C** – skał magmowych z podłoża prekambryjskiego NE Polski (źródło danych: Krzemińska i in., 2017); **D** – populacji ksenokryształów rozpoznanych w regionie łysogórskim (diabaz z Janowic); **E** – populacji ksenokryształów rozpoznanych w regionie kieleckim (tuf z Kielc i lamprofir z Podkranowa).
Age [Ma] – wiek [mln lat], Pb-Pb age [Ma] – wiek Pb-Pb [mln lat], number – liczebność, magmatic zircon – cyrkon magmowy, zircon xenocrysts – ksenokryształy cyrkonu, zircon xenocrysts – ksenokryształy cyrkonu, Precambrian basement – podłoże prekambryjskie

Małopolska Block with Kielce Region and Łysogóry Block, that documents their close relationship during Late Carboniferous to early Permian time.

The dominant group of zircon grains from lamprophyre and diabase yielded a significantly older age of crystallization. This xenocryst category derived from Paleozoic and Proterozoic sources. The early Devonian grains with concordia T-W age at 403 ±18 Ma (n = 3) are *c.* 100 Ma older than the youngest concordant grains in Podkranów, and most probably reflect contamination by local rocks in the Kielce Region. However, zircon xenocrysts recognized in the Janowice (Łysogóry Region) with ages grouping at 418 ±9.4 Ma

requires careful explanation because of the lower intercept age. It would be a potentially synchronous impulse recorded within rocks from Łysogóry Region, but comparable to the magmatic episodes widespread along Kielce Region at the Sylurian/Devonian transition.

The samples from both of regions contain some zircon produced by Late Proterozoic-Cambrian magmatic activity between 650–550 Ma (Fig. 6D, E). They correspond with the time frame of magmatism at the margin of Cadomian arc reported from the Małopolska Block (Żelaźniewicz *et al.*, 2009). In the case of Janowice diabase from Łysogóry Region, another source is suggested. At *ca.* 570–550 Ma, the volcanic activity resulting from the final stages the Rodinia break-up was widespread along the SW margin of Baltica (Shumlyanskyy *et al.*, 2016). The numerous lava flows with pyroclastic layers are known from Volyn and eastern Poland (SW margin of Baltica). Similarly, the older material and xenocrysts with an age of *ca.* 1948, *ca.* 1585, *ca.* 1634 Ma most probably derived from Baltica (Fig. 6C, D).

In contrast to the oldest xenocrysts detected in the Kielce Region (Podkranów), which display $^{207}Pb/^{206}Pb$ ages of *ca.* 2760 and *ca.* 2618 Ma, indicating a Neoarchean magmatic source rocks that are exotic (Fig. 6C vs 6E) for SW margin of Fennoscandia (Krzemińska *et al.*, 2017), rocks with age of 2.7–2.6 Ga are widespread within the inner part the Sarmatia Block (Bogdanova *et al.*, 2008; Shumlyanskyy *et al.*, 2016). The origin of xenocrysts in the range from *ca.* 2106 to *ca.* 1533 Ma, with a range of 1035–1078 Ma was usually discussed as Baltican (Belka *et al.*, 2002; Nawrocki *et al.*, 2007).

CONCLUDING REMARKS

The U-Pb zircon geochronology for volcanic rock, diabase and lamprophyre veins is less precise than previous Ar-Ar thermochronology, but allows us to decipher more than one magmatic event in the region that is a significant achievement of this contribution. The studied collection of zircon grains from the HCM magmatic rocks represent complex populations composed of the autocrysts, antecrysts, and abundant xenocrysts. They show multiple magma pulses:

1. Late Caledonian prominent magmatic events, deciphered from zircons in the Kielce tuff (Kielce Region) from autocrysts at 425.7 ±6.6 Ma and from antecrysts at 414.5 ±6.6 Ma).
2. The extensive Late Variscan magmatism in Kielce and Łysogóry regions, that occurred at 322 ±12 Ma and at 300 ±10 Ma, when the lamprophyre of Podkranów (Kielce Region) and diabase of Milejowice (Łysogóry Region) were emplaced, coeval with the silicic igneous magmatism at southern margin of Małopolska Block, which document synchronicity of magmatic events between both domains.

The zircon xenocrysts abundant in Podkranów lamprophyre (Kielce Region) as well as Janowice diabase (Łysogóry Region), incorporated into the host magma from the surrounding crust during magma ascent, confirm the identity of the detritus between the Łysogóry and Baltica crust, but derivation from Baltica sources from older grains in Kielce Region is not so obvious. The input of Cadomian grains is characteristic for the rocks from the Małopolska Block.

In memoriam Wacław Ryka (1931–1996), Zbigniew Rubinowski (1929–1997), Zbigniew Kowalczewski (1938–2018).

REFERENCES

BELKA Z., VALVERDE-VAQUERO P., DÖRR W., AHRNDT H., WEMMER K., FRANKE W., SCHÄFER J., 2002 – Accretion of first Gondwana-derived terranes at the margin of Baltica. *In*: Palaeozoic Amalgamation of Central Europe (eds. J.A. Winchester *et al.*). *Geol. Soc., London, Sp. Publ.*, **201**: 19–36.

BLACK L.P., KAMO S.L., ALLEN C.M., DAVIS D.W., ALEINIKOFF J.N., VALLEY J.W., MUNDIL R., CAMPBELL I.H., KORSCH R.J., WILLIAMS I.S., FOUDOULIS C., 2004 – Improved $^{206}Pb/^{238}U$ microprobe geochronology by the monitoring of a trace-element-related matrix effect; SHRIMP, ID–TIMS, ELA–ICP–MS and oxygen isotope documentation for a series of zircon standards. *Chem. Geol.*, **205**: 115–140.

BOGDANOVA S.V., BINGEN B., GORBATSCHEV R., KHERASKOVA T.N., KOZLOV V.I., PUCHKOV V.N., VOLOZH YU.A., 2008 – The East European Craton (Baltica) before and during the assembly of Rodinia. *Prec. Res.*, **160**: 23–45.

CASSATA W.S., RENNE P.R., SHUSTER D.L., 2009 – Argon diffusion in plagioclase and implications for thermochronometry: A case study from the Bushveld Complex, South Africa. *Geochim. et Cosmochim. Acta*, **73**: 6600–6612.

COHEN K.M., FINNEY S.C., GIBBARD P.L., FAN J.-X., 2013 (updated) – The ICS International Chronostratigraphic Chart. *Episodes*, **36**: 199–204.

CZARNOCKI J., 1919 – Stratygrafia i tektonika Gór Świętokrzyskich. Stratygrafia i tektonika staropaleozoicznych utworów Gór Świętokrzyskich (kambr, sylur, dewon dolny). *Pr. Tow. Nauk. Warszaw.*, **28**: 1–172.

DADLEZ R., 2001– Holy Cross Mts. area – Crustal structure, geophysical data and general geology. *Geol. Quart.*, **45**, 2: 99–106.

DICKINSON W.R., GEHRELS G.E., 2009 – Use of U-Pb ages of detrital zircons to infer maximum depositional ages of strata: A test against a Colorado Plateau Mesozoic database. *Earth Planet. Sci. Lett.*, **288**: 1/2: 115–125.

HANCHAR J.M., WATSON E.B., 2003 – Zircon saturation thermometry. *In*: Zircon (eds. J.M. Hanchar, P.W.O. Hoskin), *Rev. Miner. Geochem.*, **53**: 89–112.

KARDYMOWICZ I., 1967 – Intruzje mniejsze Gór Świętokrzyskich. *Biul. Inst. Geol.*, **197**: 329–412.

KELLEY S., 2002 – K-Ar and Ar-Ar dating. *Rev. Miner. Geochem.*, **47**: 785–818.

KOWALCZEWSKI Z., 2004 – Geological setting of the Milejowice-Janowice diabase intrusion: insights into post-Caledonian magmatism in the Holy Cross Mts., Poland. *Geol. Quart.*, **48**, 2: 135–146.

KOZŁOWSKI W., DOMAŃSKA-SIUDA J., NAWROCKI J., 2014 – Geochemistry and petrology of the Upper Silurian greywackes from the Holy Cross Mountains (central Poland): implications for the Caledonian history of the southern part of the Trans-European Suture Zone (TESZ). *Geol. Quart.*, **58**, 2: 311–336.

KRZEMIŃSKA E., KRZEMIŃSKI L., PETECKI Z., WISZNIEWSKA J., SALWA S., ŻABA J., GAIDZIK K., WILLIAMS I.S., ROSOWIECKA O., TARAN L., JOHANSSON Å., PÉCSKAY Z., DEMAIFFE D., GRABOWSKI J., ZIELIŃSKI G., 2017 – Mapa geologiczna podłoża krystalicznego polskiej części platformy wschodnioeuropejskiej 1 : 1 000 000. Państw. Inst. Geol., Warszawa.

KRZEMIŃSKI L., 2004 – Geochemical constraints on the origin of the mid-Palaeozoic diabases from the Holy Cross Mts. and Upper Silesia, southeastern Poland. *Geol. Quart.*, **48**, 2: 147–158.

LUDWIG K.R., 2003– User's manual for Isoplot 3.00. A geochronological toolkit for Microsoft Excel. *Berkeley Geochron. Cent. Sp. Publ.*, **4a**, (Berkeley, CA).

LUDWIG K.R, 2009 – SQUID 2: A User's Manual, rev. 12 Apr., 2009. *Berkeley Geochron. Cent. Sp. Publ.*, **5**: 1–110.

MALEC J., 2001 – Sedimentology of deposits from around the Late Caledonian unconformity in the western Holy Cross Mts. *Geol. Quar.*, **45**, 4: 397–415.

MAZUR S., PORĘBSKI S.J., KĘDZIOR A., PASZKOWSKI M., PODHALAŃSKA T., POPRAWA P., 2018 –Refined timing and kinematics for Baltica–Avalonia convergence based on the sedimentary record of a foreland basin. *Terra Nova*, **30**: 8–16.

McDOUGALL I., HARRISON T.M., 1999 – Geochronology and Thermochronology by the ^{40}Ar/^{39}Ar Method. Oxford University Press On Demand.

McKAY M.P., WEISLOGEL A.L., FILDANI A., BRUNT R.L., HODGSON D.M., FLINT S.S., 2015 – U-Pb zircon tuff geochronology from the Karoo Basin, South Africa: Implications of zircon recycling on stratigraphic age controls. *Int Geol. Rev.*, **57**: 393–410.

MIGASZEWSKI Z.M., 2002 – Datowanie diabazów i lamprofirów świętokrzyskich metodą K-Ar i Ar-Ar. *Prz. Geol.*, **50**: 227–229.

MIKULSKI Z.S., KRZEMIŃSKA E, CZUPYT Z., 2016 – The δ^{18}O isotope composition & U-Pb geochronology on SHRIMP IIe/MC. An example from the foreland of the Variscan orogenic belt (S Poland). 8th SHRIMP Workshop, Granada 6–10 September 2016, Abstract book: 77–79.

MILLER J.S., MATZEL J.E.P., MILLER C.F., BURGESS S.D., MILLER R.B., 2007 – Zircon growth and recycling during the assembly of large, composite arc plutons. *J. Volcan. Geoth. Res.*, **167**: 282–299.

NARKIEWICZ M., GRAD M., GUTERCH A., JANIK T., 2011 – Crustal seismic velocity structure of southern Poland: Preserved memory of a pre-Devonian terrane accretion at the East European Platform margin. *Geol. Mag.*, **148**: 191–210.

NAWROCKI J., DUNLAP J., PÉCSKAY Z., KRZEMIŃSKI L., ŻYLIŃSKA A., FANNING M., KOZŁOWSKI W., SALWA S., SZCZEPANIK Z., TRELA W., 2007 – Late Neoproterozoic to Early Palaeozoic palaeogeography of the Holy Cross Mountains (Central Europe): An integrated approach. *J. Geol. Soc.*, **164**: 405–423.

NAWROCKI J., KRZEMIŃSKI L., PAŃCZYK M., 2010 – ^{40}Ar-^{39}Ar ages of selected rocks and minerals from the Kraków–Lubliniec Fault Zone, and their relation to the Paleozoic structural evolution of the Małopolska and Brunovistulian terranes (S Poland). *Geol. Quart.*, **54**, 3: 289–300.

NAWROCKI J., SALWA S., PAŃCZYK M., 2013 – New ^{40}Ar-^{39}Ar age constrains for magmatic and hydrothermal activity in the Holy Cross Mts. (southern Poland). *Geol. Quart.*, **57**, 3: 551–560.

RUBINOWSKI Z., 1962 – Lamprofiry okolic Daleszyc i związane z nimi przejawy mineralizacji. *Kwart. Geol.*, **6**, 3: 245–270.

RYKA W., 1957 – Nowe spostrzeżenia dotyczące diabazu z Barda (Góry Świętokrzyskie). *Kwart. Geol.*, **1**, 2: 329–352.

SHUMLYANSKYY L., NOSOVA A., BILLSTRÖ K., SÖDERLUND U., ANDREASSON P.G., KUZMENKOVA O., 2016 – The U–Pb zircon and baddeleyite ages of the Neoproterozoic Volyn Large Igneous Province: Implication for the age of the magmatism and the nature of a crustal contaminant. *Geologiske Foreningen Forhandlinger*, **138**: 17–30.

STACEY J.S., KRAMERS J.D., 1975 – Approximation of terrestrial lead evolution by a two stage model. *Earth Planet. Sci. Lett.*, **26**: 207–221.

TRELA W., BĄK E., PAŃCZYK M., 2018 – Upper Ordovician and Silurian ash beds in the Holy Cross Mountains, Poland: Preservation in mudrock facies and relation to atmospheric circulation in the Southern Hemisphere. *J. Geol. Soc.*, **175**: 352–360.

WALCZAK A., BELKA Z., 2017 – Fingerprinting Gondwana versus Baltica provenance: Nd and Sr isotopes in Lower Paleozoic clastic rocks of the Małopolska and Łysogóry terranes, southern Poland. *Gondw. Res.*, **45**: 138–151.

WIEDENBECK M., ALLÉ P., CORFU F., GRIFFIN W.L., MEIER M., OBERLI F., von QUADT A., RODDICK J.C., SPIEGEL W., 1995 – Three natural zircon standards for U-Th-Pb, Lu-Hf, trace-element and REE analyses. *Geostand. Newslett.*, **19**: 1–23.

ŻELAŹNIEWICZ A., PAŃCZYK M., NAWROCKI J., FANNING C.M., 2008 – A Carboniferous/Permian, calc-alkaline, I-type granodiorite from the Małopolska Block, Southern Poland: implications from geochemical and U-Pb zircon age data. *Geol. Quart.*, **52**, 4: 301–308.

ŻELAŹNIEWICZ A., BUŁA Z., FANNING M., SEGHEDI A., ŻABA J., 2009 – More evidence on Neoproterozoic terranes in Southern Poland and southeastern Romania. *Geol. Quart.*, **53**, 1: 93–124.

STRESZCZENIE

Obszar Gór Świętokrzyskich jest zlokalizowany na styku dwóch bloków strukturalnych. Znajduje to swój wyraz w pewnej odrębności regionów kieleckiego i łysogórskiego. W obrębie paleozoicznych sukcesji skał osadowych znanych jest szereg wystąpień diabazów, lamprofirów oraz warstw piroklastycznych. Stanowią one punkty odniesienia, służące do korelowania osadów i epizodów magmowych w skali obu regionów. Wyniki datowania radiometrycznego przejawów magmatyzmu, obok badań biostratygraficznych i paleomagnetycznych, stanowią jeden z argumentów w trwającej dyskusji na temat wspólnej lub odrębnej historii ewolucji geotektonicznej regionu łysogórskiego i świętokrzyskiego, dla których wskazuje się, odpowiednio, jedno waryscyjskie piętro strukturalne albo dwa piętra – kaledońskie i waryscyjskie. Dotychczas wiek aktywności magmowej był tu oznaczany na całej skale lub na koncentratach mineralnych (biotyt, plagioklaz) metodą K-Ar i Ar-Ar, a daty interpretowano jako wiek krystalizacji skały. W niniejszej pracy przedstawiono nowe wyniki badań geochronologicznych, które są efektem analiz cyrkonu na mikrosondzie jonowej z zastosowaniem metody U-Pb. Wybrane do badań próbki pochodzą z obu regionów. Region łysogórski reprezentuje diabaz z wiercenia Janowice-2, a z regionu kieleckiego wytypowano lamprofir z Podkranowa oraz próbkę tufu z Kielc.

Ziarna cyrkonu wyseparowane ze skał żyłowych i z warstw piroklastycznych zwykle nie stanowią jednorodnej populacji wiekowej. Koncentraty mogą zawierać więcej grup różniących się genezą. Jedną z grup są ksenokryształy, czyli wyraźnie starsze składniki egzotyczne, inkorporowane z otoczenia podczas podnoszenia się magmy. Ponadto występują autokryształy krystalizujące na przykład w trakcie erupcji, oraz grupa antekryształów, ziaren pochodzących z wcześniejszej fazy magmatyzmu, które następnie zostały włączone do późniejszego epizodu magmowego. Zwykle złożona populacja ziaren komplikuje z jednej strony interpretację wyników badań geochronologicznych, jeśli ich celem jest wyłącznie określenie wieku magmatyzmu. Z drugiej strony, obecność kilku grup ziaren cyrkonu poszerza zakres informacji o ich skałach macierzystych, gdyż pozwala na datowanie nie tylko wieku krystalizacji skały będącej końcowym produktem magmatyzmu. Rozpoznane za pomocą katodoluminescencji SEM-CL cechy budowy wewnętrznej kryształów cyrkonu, obok ich morfologii, pozwoliły wyodrębnić różne genetycznie typy ziaren: autokryształy, ante-

kryształy i ksenokryształy. W tufie z Kielc dominują wydłużone euhedralne ziarna cyrkonu charakterystyczne dla krystalizacji wulkanicznej. Ich wiek kumuluje się w dwóch grupach. Najmłodsza (autokryształy) wskazuje na krystalizację na przełomie syluru i dewonu ok. 414,5 ±6,6 mln lat temu. Ponadto liczna populacja antekryształów o wieku 425,7 ±6,6 mln lat rejestruje epizod wcześniejszy o 10 mln lat. Oba te wyniki udokumentowane w warstwie tufu z Kielc dość dobrze korelują się z publikowanymi datami Ar-Ar, w tym z wiekiem diabazów z Zarobin ok. 415,5 ±2 mln lat oraz z Zalesia 424 ±6 mln lat, wpisując się w ramy kaledońskiej aktywności tektono-magmowej regionu kieleckiego. Pomimo nielicznych autokryształów cyrkonu w lamprofirze z Podkranowa (region kielecki) i diabazie z Janowic (region łysogórski), udało się określić czas ich krystalizacji, odpowiednio ok. 322 ±12 mln lat (n=3) i przypuszczalnie ok. 300 ±10 mln lat (n=1). W obu przypadkach jest to magmatyzm późnowaryscyjski, znany zarówno na obszarze kieleckim, jak i łysogórskim. Intruzje skał żyłowych nie pojawiały się jednocześnie; istotne okazały się tu korelacje regionalne. Wiek diabazu z Janowic (region łysogórski) jest analogiczny do wieku magmatyzmu w południowej części bloku małopolskiego, znanego z intruzji granitoidów i wulkanizmu wzdłuż strefy Kraków–Lubliniec, między 305,2 ±1,5 mln lat a 292 ±4,5 mln lat.

Osobnym zagadnieniem są populacje ksenokryształów w każdej z próbek. Zarówno w regionie kieleckim, jak i łysogórskim występują liczne ziarna kaledońskie, tworzące grupy z wiekiem konkordii ok. 403 ±18 mln lat (Podkranów) i 418 ±10 mln lat (Janowice). Szczególnie częste w regionie kieleckim są też ziarna kadomskie, prawdopodobnie pochodzące z południowej części podłoża krystalicznego bloku małopolskiego. Grupę najstarszych ksenokryształów, zwłaszcza ze skał regionu łysogórskiego, charakteryzują wieki typowe dla skorupy podłoża krystalicznego Baltiki w rejonie strefy Teisseyre'a-Tornquista. W przypadku najstarszych ziaren z regionu kieleckiego ich pochodzenie nie jest równie oczywiste. Nowe wyniki datowań pokazują, że geochronologia U-Pb na pojedynczych ziarnach cyrkonu ze skał piroklastycznych (warstwy tufów) czy żyłowych (diabaz, lamprofir) może być mniej precyzyjna niż powszechnie stosowana termogeochronologia Ar-Ar. Dostarczyła jednak bogatszych danych o geologicznej ewolucji skał macierzystych, co jest znaczącym osiągnięciem przeprowadzonych analiz.